DIMUON PRODUCTION AT THE I.S.R.

F. Vannucci
Laboratoire de Physique des Particules (LAPP)
Annecy, France

Abstract

Results from an experiment studying $pp \to \mu^+\mu^- X$ at the ISR are presented. With about 12000 muon pairs the mass spectrum extends up to 20 GeV. The data is analysed to extract the dependences on the Feynman variable X, the transverse momentum p_t and the decay angle θ. Associated hadron multiplicities are given, and an evidence for the 2 γ process in pp collisions is presented.

Résumé

Les résultats d'une experience mesurant $pp \to \mu^+\mu^- X$ aux ISR sont présentés. Avec environ 12000 paires de muons, les données permettent l'extraction des dépendences en fonction de la variable X de Feynman, de l'impulsion transverse p_t et de l'angle de desintegration θ. La multiplicité des hadrons associés est donnée, et une première évidence de l'effet á 2 photons en collision pp est presentée.

The experiment R209 studied the reaction

$$pp \rightarrow \mu^+\mu^- X$$

at the ISR. An integrated luminosity of 1.11 $10^{38}cm^{-2}$ was collected at the maximum energy of $\sqrt{s}$ = 62 GeV. About 12000 muon pairs with an invariant mass larger than 2.8 GeV were obtained.

The Detector

The apparatus is shown in Fig. 1[1]. It is composed of seven magnetized iron toroids surrounding the interaction region. The iron is at the same time the hadron absorber and the carrier of the magnetic field (1.75 T). The muons are identified by penetration, requiring a minimum of 1.8 GeV/c momentum. The absorber starts 40 cm from the interaction, thus minimizing background from π and K decays.

Large size drift chambers (up to 6.5 x 2.7 m^2) in between and around the toroids detect the muon trajectories. Immediately around the intersection a vertex detector made of modular drift chambers measures the direction of associated charged hadrons.

Three layers of scintillator counters in coincidence form a candidate muon track. The trigger requires two tracks at an angle $180^o \pm 50^o$ in the non-bending plane. With a luminosity of $10^{31}cm^{-2}s^{-1}$ the trigger rate is about 1 per second.

Mass Spectrum

Fig. 2 shows the cross section for dimuon production with masses above 4 GeV. The distribution is fitted to the sum of the contributions expected from the Υ resonances and from the Drell-Yan continuum.

The Υ signal is in agreement with the experimental resolution $\Delta m/m \simeq$ 11% consequence of multiple scattering in iron. The total production cross section for $\Upsilon + \Upsilon' + \Upsilon''$ is found to be:

$$B_{\mu\mu}\sigma = (14 \pm 3.5)\ 10^{-36}cm^2.$$

Three very high mass events are seen in the plot. They enable a 2σ upper limit to be set on resonance production with mass above 20 GeV.

$$B_{\mu\mu}\sigma < 40\ 10^{-38}cm^2.$$

The continuum is fitted by the scaling expression:

$$m^3 \frac{d\sigma}{dm} = (7.7 \pm 0.4)\ 10^{-33}\ \frac{(1-\sqrt{\tau})^{10}}{\sqrt{\tau}}\ \ GeV^2cm^2,$$

where $\tau = m^2/s$. This form also fits the CFS[2] results. This is not a test of scaling because the CFS data cover the range $0.2 < \sqrt{\tau} < 0.5$ while the present data are in the range $0.05 < \sqrt{\tau} < 0.2$: the overlap is small but we have now a single phenomenological expression which accounts for all data in the extended range $0.05 < \sqrt{\tau} < 0.5$.

It is interesting to note that a fit using the structure functions of the hadron recently measured at CERN[3] describes our low mass (below T) region without the need of a K factor larger than one. But those structure functions have been measured in a region of $\sqrt{\tau}$ which corresponds to our high mass data, where a factor $K \tilde{=} 2$ can be accomodated.

Dynamics of the Dimuon Pairs

(a) Due to its asymmetric configuration the detector covers a large region in the variable Feynman X. This allows the extraction of the X dependence with good accuracy. In the mass range 5 to 8 GeV we find $(1 - |X|)^{2.9\pm0.3}$ In the mass range including the T we find $(1 - |X|)^{3.2\pm0.3}$.

(b) Due to the alignment of fermion spins in the Drell-Yan mechanism one expects an angular distribution of one muon in the dimuon system compatible with $1 + \cos^2\theta$. The analysis has been done in the Collins-Soper[4] frame. In the region $6 < m < 8$ GeV the result is $1 + (1.6\pm0.7)\cos^2\theta$. In the mass region which includes the T resonances the distribution is $1 + (0.3\pm0.6)\cos^2\theta$ compatible with being flat.

(c) The p_t dependence of the dimuons has been extracted. In the mass range 6 to 8 GeV it is

$$e^{-(1.26\pm0.11)p_t} = \frac{1}{p_t}\ \frac{d\sigma}{dp_t},$$

in the higher mass range 8 to 11 GeV it is

$$e^{-(1.18\pm0.10)p_t} = \frac{1}{p_t}\ \frac{d\sigma}{dp_t}.$$

This gives high values of $\langle p_t \rangle$ shown in Fig. 3, where results of previous experiments[5] are also plotted. For a given mass, $\langle p_t \rangle$ clearly increases with $\sqrt{s}$ as fast as linearly. This is in contradiction with the simple

Drell-Yan model and gives support to the need of higher order QCD diagrams involving gluons[6].

Associated Hadrons

(a) The vertex detector immediately surrounding the intersection region reconstructs charged particles produced together with the muon pair analysed in the outer spectrometer. Due to the lack of magnetic field it only measures the direction of particles.

The total multiplicity of associated hadrons decreases monotonically with the energy carried away by the dimuon system. More interestingly, as shown in Fig. 4, the multiplicity of hadrons in the hemisphere away from the dimuon increases with increasing p_t, while the multiplicity in the hemisphere toward the dimuon does not depend on p_t. This again gives support to the idea that high p_t dimuons arise from gluon interactions, and the high p_t is balanced by an opposite jet[6].

(b) The multiplicity of associated charged hadrons for all dimuon events is presented in Fig, 5. The histogram shows two obvious contributions. The bulk of the data has a distribution with a maximum around 11. This distribution fails to account for about 100 events which do not have any hadrons in the vertex detector accompanying the dimuon. Those hadronless events (1% of the whole statistics) tend to reconstruct low masses and low p_t. The most natural interpretation assigns those events to the two photon process. This is corroborated by the magnitude of the cross section[7], $10^{-35} cm^2$ for a mass of 3 GeV which is indeed in agreement with the computation of this process never detected previously in hadronic collisions.

References

1) Work performed by the CERN-Harvard-LAPP-MIT-Naples-Pisa Collaboration: D. Antreasyan, W. Atwood, V. Balakin, R. Battiston, U. Becker, C. Bellettini, P.L. Braccini, J.G. Branson, J. Burger, F. Carbonara, R. Carrara, R. Castaldi, V. Cavasinni, F. Cervelli, M. Chen, G. Chiefari, T. Del Prete, E. Drago, M. Fujisaki, M. Hodous, T. Lagerlund, P.Laurelli, O. Leistam, R. Little, P.D. Luckey, M.M. Massai, T. Matsuda, L. Merola, M. Morganti, M. Napolitano, H. Newman, D. Novikoff, L. Perasso,

K. Reibel, J.P. Revol, R. Rinzivillo, G. Sanguinetti, C. Sciacca, P. Spillantini, M. Steuer, K. Strauch, S. Sugimoto, S.C.C. Ting, W. Toki, M. Valdata-Nappi, C. Vannini, F. Visco and S.L. Wu.

2) J.K. Yoh et al., Phys. Rev. Lett. 41, 684 (1978).

3) H. Decamp, Proceedings of this Conference.

4) J.C. Collins & D.E. Soper, Phys. Rev. D16, 2219 (1977).

5) J.G. Branson et al., Phys. Rev. Lett. 38, 457 (1977).

L.M. Lederman, Proc. 19th Int. Conf. on High-Energy Physics, Tokyo, 1978, p. 706.

6) See for instance: Ed. Berger, Proceedings of this Conference.

7) M.S. Chen et al., Phys. Rev. D7, 11 (1973).

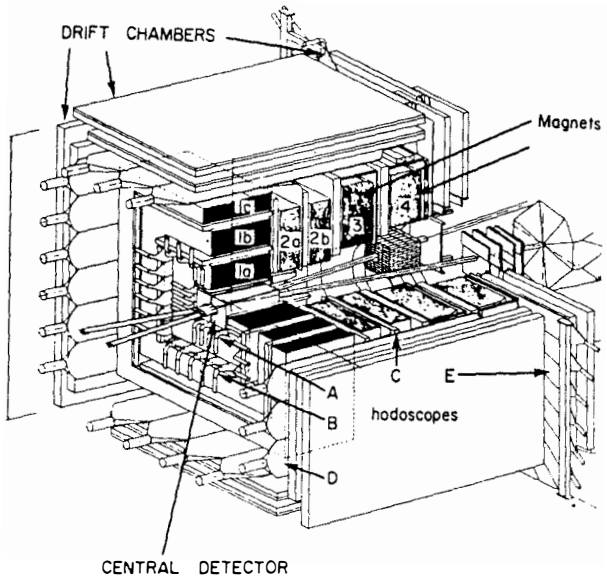

Figure 1

Artistic view of the detector with a cut-out showing the internal structure.

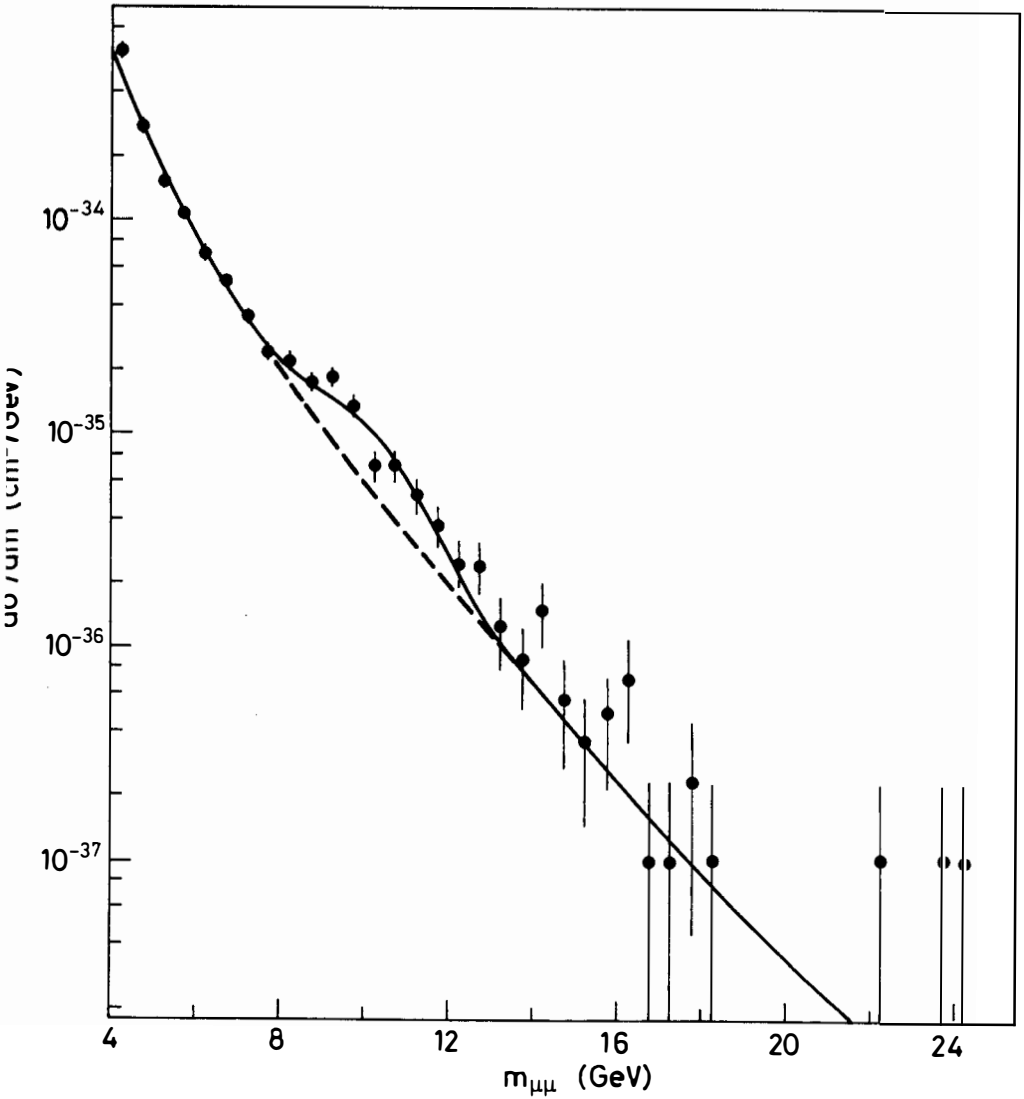

Figure 2

Measured dimuon cross section at $\sqrt{s}$ = 62 GeV.
The solid line represents a fit of the continuum
with contribution from the T resonances.

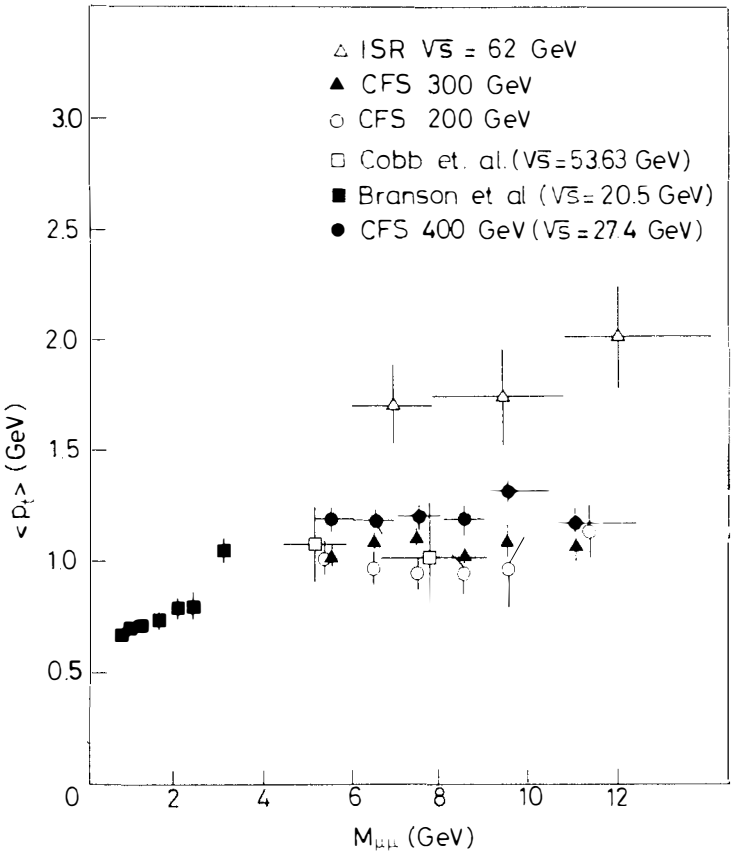

Figure 3

$\langle p_t \rangle$ as a function of the dimuon mass with results from FNAL and the I.S.R.

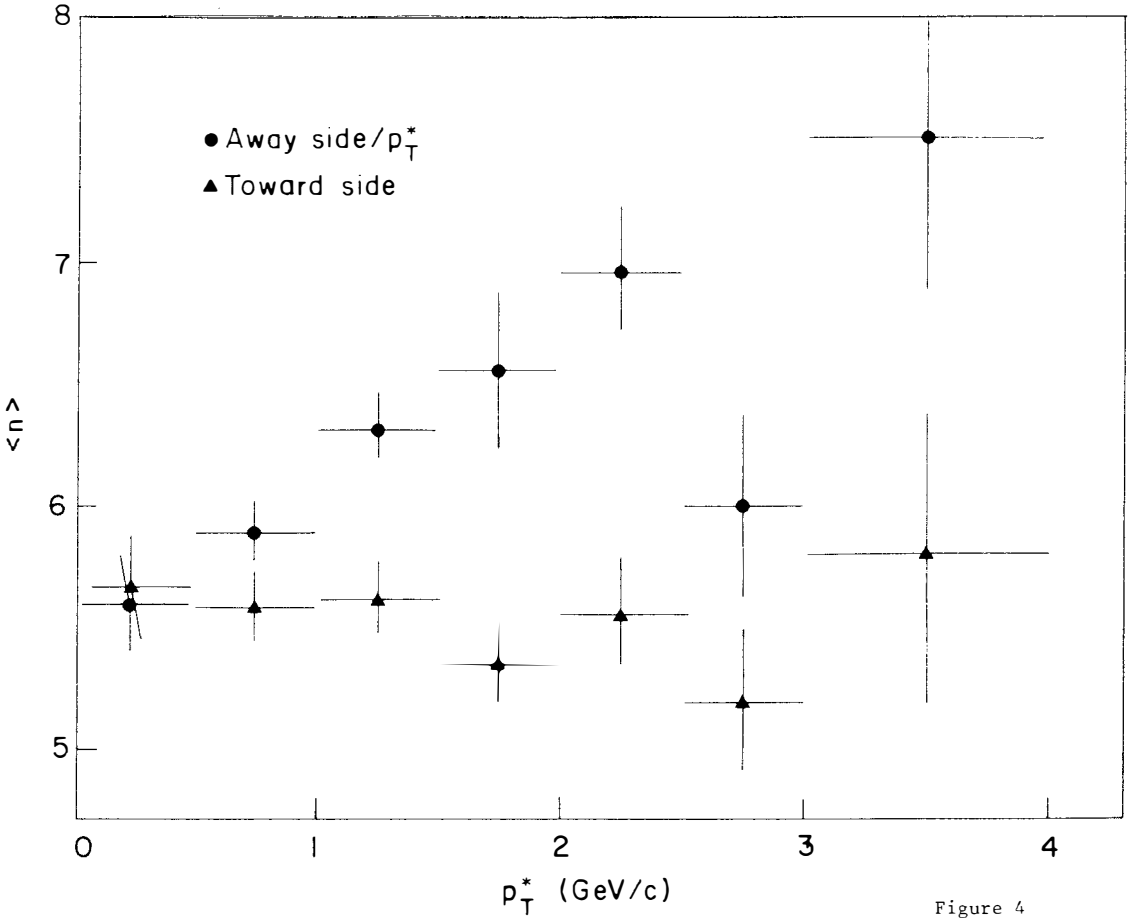

Figure 4

Multiplicity of charged tracks as a function of the dimuon transverse momentum, for the two hemispheres away and toward the dimuon system.

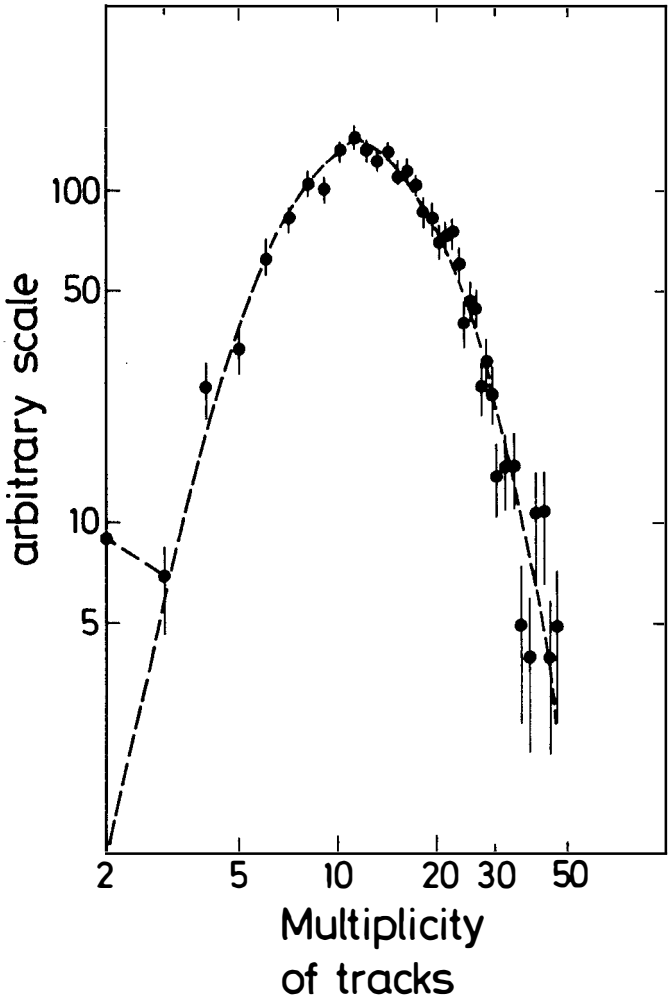

Figure 5

Multiplicity plot for the charged tracks seen in dimuon events, the two muons are included.